

Efficient parameter assessment of different-sized photovoltaic modules for performance evaluation

LAMRINI, Nassim, OUFETTOUL, Hicham, EL BARKOUKI, Bouthaina, AIT ABDELMOULA, Ibtihal, EL MEDHDI, Abdelmalek, BOUGROUN, Zineb and ISSA, Walid <<http://orcid.org/0000-0001-9450-5197>>

Available from Sheffield Hallam University Research Archive (SHURA) at:

<https://shura.shu.ac.uk/33892/>

This document is the Accepted Version [AM]

Citation:

LAMRINI, Nassim, OUFETTOUL, Hicham, EL BARKOUKI, Bouthaina, AIT ABDELMOULA, Ibtihal, EL MEDHDI, Abdelmalek, BOUGROUN, Zineb and ISSA, Walid (2024). Efficient parameter assessment of different-sized photovoltaic modules for performance evaluation. In: Digital Technologies and Applications : Proceedings of ICDDTA'24, Benguerir, Morocco. Lecture Notes in Networks and Systems, 4 . Springer, 384-397. [Book Section]

Copyright and re-use policy

See <http://shura.shu.ac.uk/information.html>

Efficient parameter assessment of different-sized photovoltaic modules for performance evaluation

Nassim LAMRINI^{1,2}, Hicham OUFETTOUL^{2,3}, Ibtihal AIT ABDELMOULA², Bouthaina EL BARKOUKI², Abdelmalek El MEHDI¹, Zineb BOUGROUN¹, and Walid ISSA⁴

¹ Smartict LAB National Schools Of Applied Sciences, Oujda, Morocco.

`hichamoufettoul@research.emi.ac.ma`

² Green Energy Park Research Platform (GEP, IRESEN/UM6P), Ben Guerir, Morocco.

³ Mohammadia School of Engineers, Mohammed V University in Rabat, 10080, Rabat, Morocco.

⁴ Engineering and Maths department, Sheffield Hallam University, Sheffield, UK

Abstract. To date, investigations into extracting photovoltaic (PV) model parameters remain a prominent and enduring area of scholarly research. The literature provides several methodologies demonstrating substantial precision, complexity, and practical relevance divergence. This investigation introduces a meta-heuristic strategy for retrieving the five parameters of the Single Diode Equivalent Model (SDM) applicable to photovoltaic modules characterized by varying cell sizes, quantities, and different PV technologies (including crystalline silicon and polycrystalline). This study has provided practical recommendations for designing innovative parameter extraction methodologies based on photovoltaic models, which are relevant for enhancing the efficiency of performance, control, detection, and diagnosis approaches for PV anomalies.

Keywords: Photovoltaic Array · single diode model · parameters extraction · failure · GWO.

1 Introduction

Solar energy is deemed sustainable and ecologically benign owing to its lesser environmental and public health ramifications than fossil fuels. The falling cost of photovoltaic modules, juxtaposed with the escalating and potentially depleting price of petrochemical fuels, has accelerated the adoption of solar PV systems. These systems, formerly considered solely for specific applications in remote and isolated areas, are now extensively used [1]. Modeling photovoltaic systems is a vital component of solar energy research, as it plays a pivotal role in their design and optimization. A comprehensive understanding of their intricate workings is indispensable in responding to the growing need for sustainable energy options [2–4]. Typically, a model representation of a photovoltaic generator incorporates an equivalent circuit and a set of parameters that accurately describe

its electrical characteristics and operational behavior. Eliciting these specifications is complex, as they are absent in the photovoltaic module's data sheet, and their values fluctuate based on varying operating conditions [5]. The precision of the parameters derived from the model holds paramount significance. Furthermore, the accuracy of the PV model is directly correlated with the quantity of integrated PV characteristics [6].

In the academic literature, five parameters, namely I_{ph} , I_s , a , R_s , and R_{sh} , are commonly utilized when applying the single-diode model. This practice simplifies the process, as the double-diode model (DDM) requires the inclusion of two diodes that present a significant number of unknown variables [7]. Nevertheless, the double-diode model replicates the process of minority carrier dispersion and recombination in photovoltaic solar cells. The fundamental methods for extracting PV model parameters are divided into three primary classes: numerical, analytic, non-iterative, and optimization strategies [8]. Numerical techniques involve solving equations through numerical calculations, trial and error, or alternative iterative algorithms. On the other hand, analytic methods use a set of equations that are resolved explicitly, simplifying both formulation and conventional implementation. The parameters are deduced through curve fitting to minimize the disparity between the theoretical and measured I-V curves in the optimization method. Furthermore, various metaheuristic algorithms fall into this category. The numerical approach requires the preliminary determination of the initial parameter values, and certain parameters may exhibit prolonged convergence times to reach the global optimum. Consequently, it is deemed unsuitable for online fault diagnosis. However, the key point positioning and sampling accuracy constrain the current analytical solution technique. Consequently, both methodologies face limitations in extracting the five parameters in a multip peaked condition induced by partial shading. The optimization technique surpasses previous methods in accuracy, and its versatility extends to online fault detection and diagnosis. Several meta-heuristic algorithms have been proposed in the literature over the last decade. For instance, the advanced approaches detailed in references [9] and [10] hinge on the application of genetic algorithms (GA) and particle swarm optimization (PSO) for the extraction of five unknown parameters. On the other hand, in this study [11, 12], the authors opted for the Differentiation Evolutionary (DE) approach and the Improved Adaptive Differential Algorithm (IADE) to extract the parameters of a single-diode model. A long PV extraction technique list is presented in the literature, such as CS, GWO, ABC... The core objective of this study is to investigate the robustness and accuracy of the proposed procedure rather than to evaluate its performance across diverse scenarios. The choice to apply the GWO algorithm is grounded in its demonstrated efficacy in literature, particularly in comparison to analogous methodologies within the same family. Furthermore, this inquiry extends to the application of the GWO algorithm across multiple photovoltaic modules, varying in sizes, technological classifications, and cell numbers within the panel.

This study aims to evaluate the algorithm's ability to preserve its efficiency and precision concerning the number of cells. This evaluation aims to provide

insights into the optimal quantity of cells required to effectively detect faults. Finally, the authors agree to present this paper comprehensively and recommend the following organization: The second section outlines the mathematical formulation of the PV array model, while the third section elaborates on the extraction parameters of the PV model, emphasizing essential performance indicators. Following this, the fourth section elucidates the approach’s implementation, offering a comprehensive description of its design and execution. In addition, section 5 details the experimental testing process. Finally, the paper includes a discussion of results with a brief conclusion, accompanied by recommendations for further investigations.

2 Mathematical formulation of PV models

2.1 Single diode model

This section briefly overviews the theoretical concepts associated with photovoltaic modeling, particularly the single-diode model. It was initially developed to mimic monocrystalline silicon photovoltaic cells. However, it has become widely used in photovoltaic modeling due to its simplicity and minimal computational requirements [4, 13]. Further advanced variants that incorporate two or three diodes to enhance accuracy at low irradiance are available [14]. Nevertheless, the primary emphasis of this study is on the single-diode model, while its equivalent circuit is presented in Fig 1. This circuit includes five parameters, which are as follows: The photocurrent (I_{ph}), the diode saturation current (I_s), the modified diode factor (a), the series resistance (R_s) and the shunt resistance (R_{sh}). The output current can be formulated as follows:

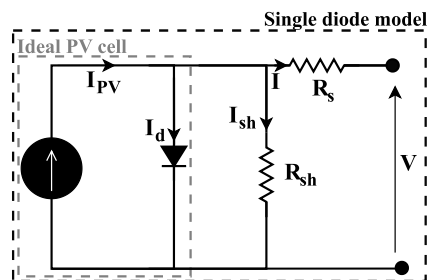


Fig. 1: PV cell’s equivalent circuit.

$$I = I_{ph} - I_d - I_{sh} \quad (1)$$

According to Shockley’s equation and Kirchoff’s voltage law, I_d and I_{sh} can be calculated as follows:

$$I_d = I_s \times \left[\exp \frac{V + I \times R_s}{a \times V_t} - 1 \right] \quad (2)$$

$$I_{sh} = \frac{q(V + I \cdot R_s)}{R_{sh}} \quad (3)$$

Where I_s denotes the diode reverse saturation current, V represents the cell output voltage, and V_t is the junction thermal voltage, formulated as outlined in Equation 4.

$$V_t = \frac{k \times T}{q} \quad (4)$$

Where k symbolizes Boltzmann's constant, T denotes the junction temperature in Kelvin ($k = 1.380650310^{-23} J/K$), and q signifies the electronic charge ($q = 1.6021764610^{-19} C$). From the above equations, the output current I becomes the following:

$$I_{cell} = I_{ph} - I_o \left[\exp \frac{V + I \cdot R_s}{V_t} - 1 \right] - \frac{V + I \cdot R_s}{R_{sh}} \quad (5)$$

Identifying these parameters is crucial to accurately simulating the actual behavior of the photovoltaic system, improving the model's ability to reflect and predict the complexities inherent in practical applications.

2.2 PV module model

The layout of a photovoltaic panel establishes a series of interconnections between a set of solar cells, with the specific aim of increasing the panel's output voltage. Similarly, photovoltaic modules can be interconnected in parallel, in series, or a combination of both interconnection schemes, as seen in Figs 2 and 3. The mathematical expression of a photovoltaic array requires considering the number of solar modules arranged in series (N_s) and parallel PV strings (N_p). The mathematical formula of a photovoltaic (PV) module is specified in Equation, where commercially available panels typically comprise cells interconnected in a series topology [15].

$$I_{module} = I_{ph} - I_o \left[\exp \left(\frac{V + I \cdot R_s \times N_s}{V_t \times N_s} \right) - 1 \right] - \frac{V + I \cdot R_s \times N_s}{N_s \times R_{sh}} \quad (6)$$

The validity and applicability of (6) are not limited to a single module, as it can be applied to any number of cells connected in series. This equation is applicable if N_{module} modules, each containing N_{cell} cells in series, are interconnected.

$$N_s = N_{cell} \times N_{module} \quad (7)$$

The equation describing the relationship between the output current (I_{array}) and voltage (V_{array}) of a photovoltaic panel, which consists of N_s cells connected in series and N_p strings connected in parallel, is as follows:

$$I_{\text{array}} = N_p \times I_{\text{PV}} - I_S \times N_p \times \left(\exp \left(\frac{q(V_{\text{module}} + \frac{N_s}{N_p} \times I_{\text{module}} \times R_s)}{K \times T \times n \times N_s} \right) - 1 \right) - \frac{V_{\text{module}} + \frac{N_s}{N_p} \times I_{\text{module}} \times R_s}{\frac{N_s}{N_p} \times R_{\text{sh}}} \quad (8)$$

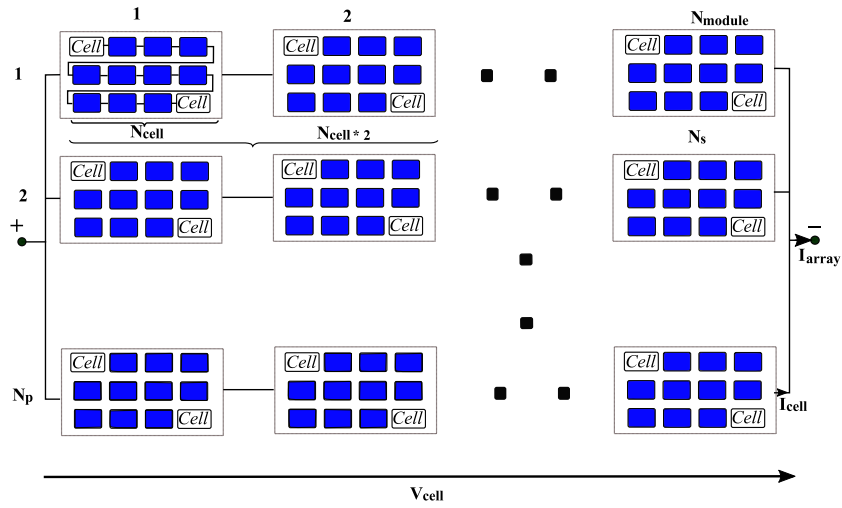


Fig. 2: Synoptic view of photovoltaic system parameters.

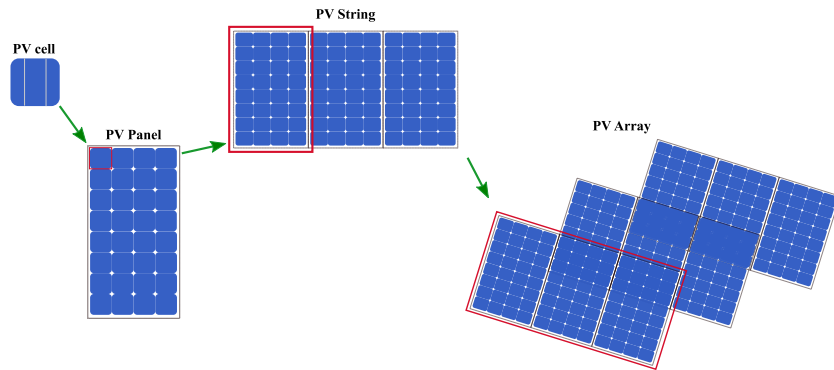


Fig. 3: Fundamental Components of PV Systems: Cells, Modules, and Arrays.

3 Extraction parameters of PV model

PV models are significant for cell performance assessment, simulation, control, and optimization. They also properly simulate PV cell current-voltage characteristics. Model precision depends on unknown parameter retrieval accuracy. Therefore, proper extraction of these traits is crucial. As parameter extraction entails acquiring experimental data, including solar irradiance, temperature, voltage, and current measurements. Consequently, an appropriate PV model and optimization algorithm are utilized to ensure alignment between the model and the collected data. This process involves iteratively refining the parameter estimates until a satisfactory level of agreement is achieved. Several key performance indicators serve the purpose of the objective function, including parameters such as the absolute individual current error (IAEC), absolute individual power error (IAEP), cumulative sum of absolute individual current error (SIAE), mean absolute error (MAE), relative error (RE), root mean square error (RMSE), and correlation coefficient, which are indispensable for meticulous assessment of prediction accuracy and reliability.

- **Individual Absolute Current Error (IAE_c):** The Individual Absolute Current Error at a given moment is the absolute difference between the calculated current ($I_{\text{calculated}}$) and the measured current ($I_{\text{experimental}}$).

$$IAE_c(t) = |I_{\text{calculated}}(t) - I_{\text{experimental}}(t)| \quad (9)$$

- **Individual Absolute power Error (IAE_p):** The Individual Absolute Power Error is the absolute difference between the measured power ($P_{\text{calculated}}$) and the desired or reference power ($P_{\text{experimental}}$) at that time:

$$IAE_p(t) = |P_{\text{calculated}}(t) - P_{\text{experimental}}(t)| \quad (10)$$

- **the sum of individual absolute current error ($SIAE$):** The Sum of Individual Absolute Current Error (SIAE) is the sum of the calculated absolute current errors. It represents the cumulative absolute discrepancy between the measured and calculated currents over a specified period.

$$SIAE = \sum_{i=1}^N IAE_{c_i} \quad (11)$$

- **Root Mean Squared Error ($RMSE$):** The Root Mean Squared Error (RMSE) measures the deviation between observed true values and estimated values.

$$RMSE = \sqrt{\frac{\sum_{i=1}^n (I_{\text{calculated}} - \hat{I}_{\text{experimental}})^2}{n}} \quad (12)$$

- **Correlation coefficient R^2 :** The correlation coefficient, labeled as R^2 , quantifies the extent to which the variation in the dependent variable can be predicted by the independent variables.

$$R^2 = 1 - \frac{\sum_{i=1}^n (\text{experimental}_i - \text{Calculated}_i)^2}{\sum_{i=1}^n (\text{experimental}_i - \overline{\text{experimental}})^2} \quad (13)$$

Where:

t : presents the specific time instance.

$I_{calculated}(t)$: is the calculated current at time t .

$I_{experimental}(t)$: is the experimental or reference current at time t .

$P_{calculated}(t)$: is the calculated power at time t .

$P_{experimental}(t)$: is the experimental or reference power at time t .

n : denotes the number of data points or samples in a dataset. In the context of RMSE, it represents the total number of observations being compared.

4 Grey wolf optimization technique

The grey wolf optimizer (GWO) selected in this study as the optimization algorithm was created by Mirjalili et al [16]. It is an innovative meta-heuristic algorithm miming grey wolves' leadership structure and hunting tactics. The GWO model consists of four main components: Alpha, Beta, Delta, and Omega grey wolves, each serving a specific function. Alpha wolves assume leadership roles and optimize their lifestyles, whereas beta wolves follow and provide assistance. Delta, representing the third-ranking class with the lowest Grey Wolf (GW) level, assumes the role of a scapegoat, while Omega represents the lowest-ranking class as shown in Fig 4. This investigation applies GWO method for

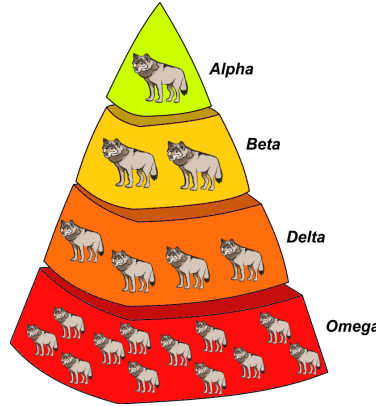


Fig. 4: Social hierarchy of wolves in the GWO.

optimizing the extraction of parameters for a single diode model. The GWO approach is comprised of three main components: encirclement, hunting, and prey attacks. The following equations illustrate the mathematical formulations utilized to elucidate the GWO approach:

- **Encircling:** Each search agent surrounds the target after detecting and pinpointing the prey location. The following mathematical model illustrates the cyclical nature:

$$\vec{A}_i = 2\vec{a}\vec{r}_1 - \vec{a} \quad (14)$$

$$\vec{C}_i = 2 \times \vec{r}_2 \quad (15)$$

Where A and C represent coefficient vectors designed to preserve an optimal equilibrium between exploration and exploitation. r_1 and r_2 are random integers ranging between $[0, 1]$. Simultaneously, the components of 'a' undergo a gradual reduction from 2 to 0 across successive iterations.

- **Hunting:** Following the positions of all agents α, β, γ , the grey wolves engaged in pursuing the prey after encircling it. The ensuing equations encapsulate the refined conceptual framework underpinning this procedure. Sure, here's the equation split into two separate equations:

$$\begin{aligned} \vec{D}_\alpha &= |\vec{C}_1 \vec{X}_\alpha(t) - \vec{X}(t)|, \\ \vec{D}_\beta &= |\vec{C}_2 \vec{X}_\beta(t) - \vec{X}(t)|, \\ \vec{D}_\delta &= |\vec{C}_3 \vec{X}_\delta(t) - \vec{X}(t)| \end{aligned} \quad (16)$$

$$\begin{aligned} \vec{d}_1 &= \vec{X}_\alpha - \vec{D}_\alpha \vec{A}_1, \\ \vec{d}_2 &= \vec{X}_\beta - \vec{D}_\beta \vec{A}_2, \\ \vec{d}_3 &= \vec{X}_\delta - \vec{D}_\delta \vec{A}_3 \end{aligned} \quad (17)$$

$$\vec{d}_{out} = \frac{\vec{d}_1 + \vec{d}_2 + \vec{d}_3}{3} \quad (18)$$

Where \vec{X} and $\vec{X}_{\alpha, \beta, \delta}$ indicate the search agent and optimum solution positions, respectively, and t denotes the number of iterations.

- **Attacking:** Grey wolves surrounded the prey and started readying themselves for the catch. When A is greater than one, the grey wolves tend to stay away from the prey and engage in global scanning. However, when A is smaller than one, the grey wolves tend to approach the prey to perform local scanning. The range of A is between $-2a$ and $2a$.

The following process is applied to the PV parameters extraction. Hence, Fig 5 depicts the GWO flowchart.

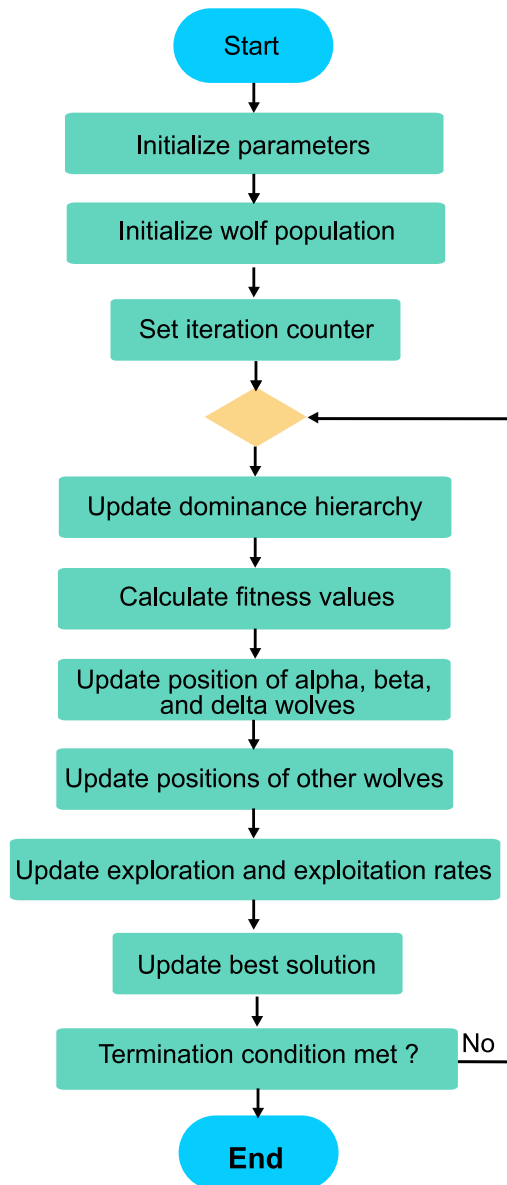


Fig. 5: Flowchart of the GWO algorithm for the PV parameter extraction application.

5 Experimental Test Process

In this section, the objective of the testing process is to collect I–V curve data for diverse PV panels of varying sizes to evaluate the applicability of the extraction algorithm across a spectrum of cells. The instrument chosen for this purpose is the I–V tracer referenced as (PVPM 1000X), renowned for its high input voltage capacity. Fig 6 shows a graphical illustration of the experimental testing process performed in this study. This procedure utilizes specific reference panels, the specifications of which are listed in Table 1. Figs 7 to 12 depict the I–V tracer schematics for these panels and outline the approach for accessing a particular PV cell number. The testing methodology incorporated a junction box of a designated panel to access the subparts of the PV module, facilitating targeted assessment of specific cell numbers, as illustrated in Fig 13.

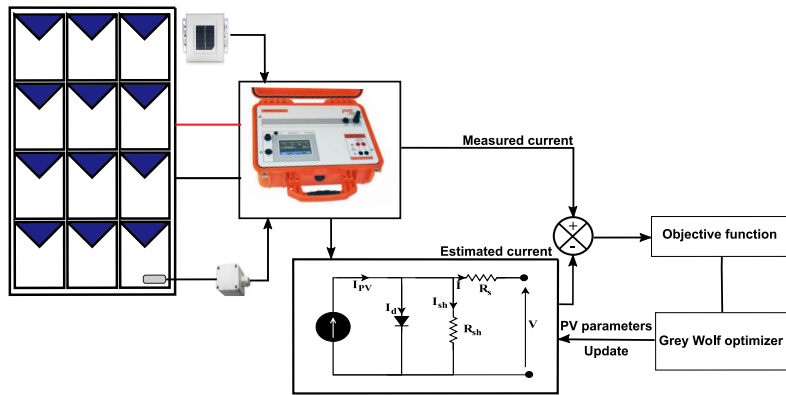


Fig. 6: Proposed strategy for extracting parameters of photovoltaic modules.

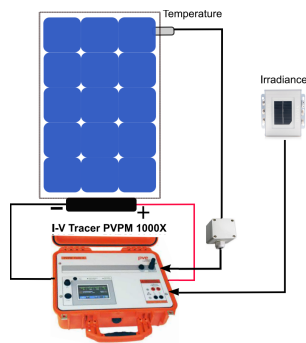


Fig. 7: First scenario with small photovoltaic panel.

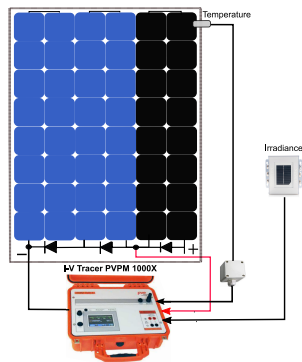


Fig.8: Second scenario where a sub-part of the photovoltaic panels is explored.

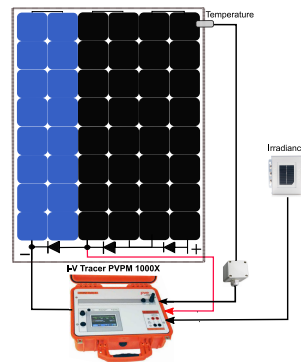


Fig.9: Third scenario where two sub-parts of the photovoltaic panels are explored.

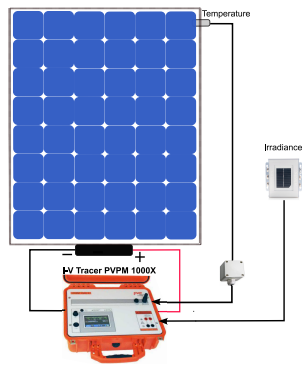


Fig.10: Fourth scenario for a single photovoltaic panel.

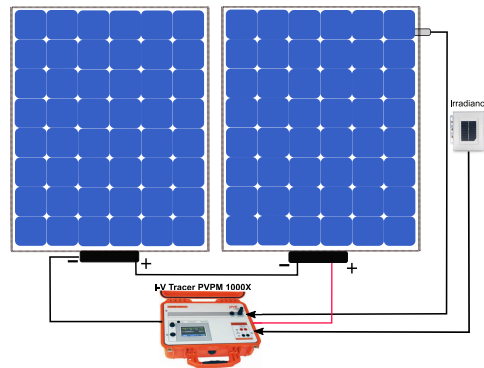


Fig.11: Fifth scenario for a two photovoltaic panel.

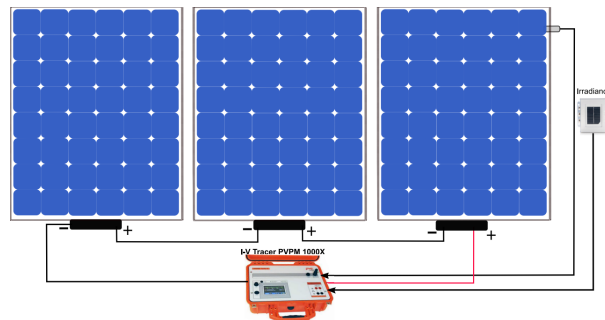


Fig.12: Sixth scenario for three photovoltaic panels.

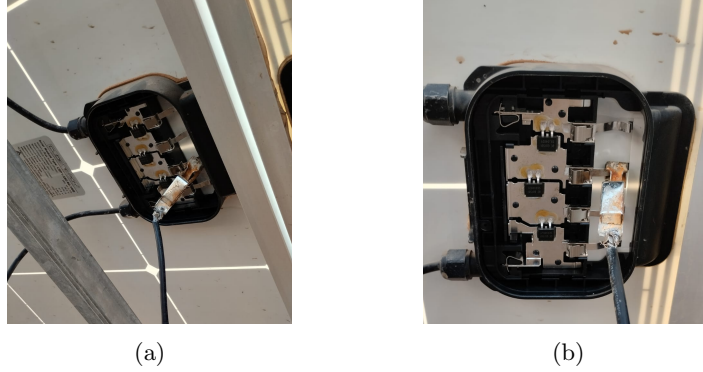


Fig. 13: Visualization of PV Panel Sub-parts Access: (a) Single sub-part interconnection figure, (b) Two sub-parts interconnection figure.

Table 1: Almaden SEA P72T polycrystalline PV panel characteristics at STC

Characteristics	Values of first Panel	Values of second Panel
Maximum Power P_{\max} (W)	280	20
Voltage at Maximum Power	31.6	17.2
V_{mpp} (V)		
Current at Maximum	8.84	1.17
Power I_{mpp} (A)		
Open Circuit Voltage V_{oc}	39	21.2
(V)		
Short Circuit Current I_{sc}	9.32	1.28
(A)		
Weight (kg)	—	—
Dimension (m)	$1.680 \times 0.99 \times 0.005$	$0.48 \times 0.35 \times 0.017$
Number of Cells	60	36

Table 2: Values of Parameters

Parameter	Scenario 1 value	Scenario 2	Scenario 3	Scenario 4	Scenario 5	Scenario 6
I_{ph}	1.228	9.601	8.339	8.347	8.907	8.787
I_{sd}	0.065	0.294	0.0001	0.0018	$5.118 \text{ e-}09$	$4.246\text{e-}11$
R_{sh}	594.724	2000	257.699	400	781	243
R_s	0.360	0.269	0.924	1.166	0.285	0.025
n	50	78.272	102.078	172.489	23.051	10.670

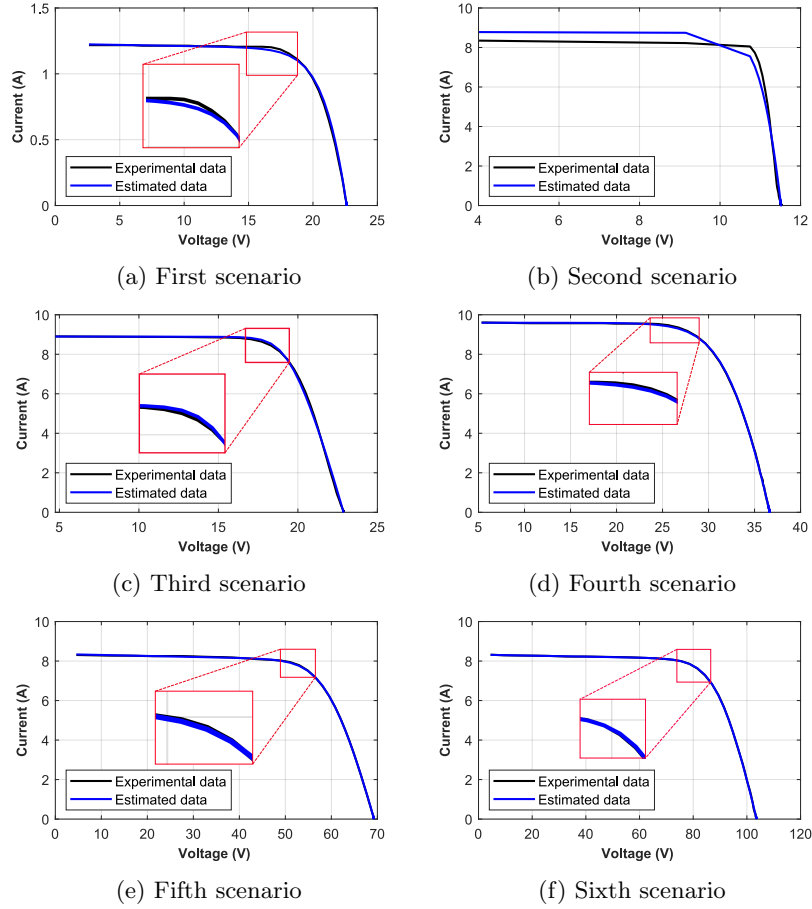


Fig. 14: Different power curve result scenarios

6 Discussion of Results

To evaluate the objective of this study, a detailed analysis was conducted, spanning from a restricted sample of individual photovoltaic cells to a more extensive array of photovoltaic strings and sub-components of PV modules. This approach allows the effectiveness of parameter extraction methodologies to be rigorously evaluated across varying scales and configurations. Our analysis relied on the key performance indicators defined in Section II, with a specific focus on the Root Mean Square Error (RMSE), which indicated values of 0.036 for the initial scenario, 1.4 for the subsequent scenario, and 0.009 for the final scenario. However, our focus in this investigation was on the discrepancy between the global maximum power point of the experimental data and the estimated data. Given the critical requirement for photovoltaic arrays to operate continuously at the

GMPP, especially in applications utilizing the Global Maximum Power Point Tracking (GMPPT) technique, this assessment was conducted using the Global Maximum Power Point (GMPP), which is deemed logical and has a significant impact. The results, illustrated in Figure 14a, reveal a significant variance in a small PV panel setup of 36 cells, emphasizing the challenges in achieving accurate parameter estimations in smaller arrays. This significant discrepancy persisted in the second scenario with a configuration of 20 cells, as shown in Figure 14b, where the gap between the estimated and actual values was also notable. However, in the third scenario, as depicted in Figure 14c, the discrepancy was markedly reduced, suggesting better model alignment with the actual measurements as the scale of the photovoltaic system increased. The fourth scenario Figure 14d further confirmed the model’s efficacy in larger PV module configurations, showing a minimal disparity between the estimated and actual data, thereby substantiating the model’s accuracy in extensive setups. The intrigue deepens in the scenarios outlined in Figures 14e and 14f, where the disparities, while still present, are minor and suggest an intriguing pattern. The model’s accuracy in the parameter estimation appears to improve as the complexity of the PV system configuration increases. This observation is crucial for applications involving complex PV arrays, where precise parameter estimation is crucial. These findings highlight the optimal performance of the model when applied to systems incorporating multiple cells interconnected by cables and soldering, which may introduce complexities such as varying series and shunt resistances. This configuration not only challenges the model but also shows its potential to reflect the intricate dynamics of real-world PV systems accurately. Ultimately, this investigation concludes that extracting photovoltaic parameters is well suited to photovoltaic modules, particularly photovoltaic strings. Its effectiveness in larger configurations especially recommends its implementation in settings where fault detection and diagnostic systems are integral to operational efficiency and system reliability. The ability of the model to adapt to the nonlinear characteristics of PV systems and effectively locate global optima under complex conditions was observed in terms of computational time and stability. Furthermore, insights gained from the variability observed in smaller system setups highlight a potential area for further research, and we suggest additional research to improve the model’s accuracy, especially in smaller or less complex systems, which would increase its adaptability across a wide range of photovoltaic technologies and installation sizes.

7 Conclusion

This paper introduces the application of a metaheuristic technique, GWO, for extracting photovoltaic parameters, which is a pivotal process within the realm of failure detection and diagnosis. Our contribution lies in advocating for the optimal scale of cell numbers required for accurate parameter extraction, which is crucial for simulating the behavior of photovoltaic panels. Furthermore, this study evaluates the efficacy of various scenarios based on disparities in the max-

imum power point (MPP) levels which a critical aspect of the PV system operating at this power point. Ultimately, this investigation is a valuable reference for researchers embarking on the detection, diagnosis, and digital twin development of PV arrays. A further improvement in this area involves the extraction of parameters during the system operation.

Acknowledgments. This work is performed in the framework of the INTELLIGENT PV Project funded by the Research Institute in Solar Energy and New Energies (IRESEN).

References

1. Oufettoul, H., Motahhir, S., Aniba, G., Masud, M., AlZain, M.A.: Improved TCT topology for shaded photovoltaic arrays. *Energy Reports* **8** (November 2022) 5943–5956
2. Victoria, M., Haegel, N., Peters, I.M., Sinton, R., Jäger-Waldau, A., del Cañizo, C., Breyer, C., Stocks, M., Blakers, A., Kaizuka, I., Komoto, K., Smets, A.: Solar photovoltaics is ready to power a sustainable future. *Joule* **5**(5) (May 2021) 1041–1056
3. Maka, A.O.M., Alabid, J.M.: Solar energy technology and its roles in sustainable development. *Clean Energy* **6**(3) (June 2022) 476–483
4. Oufettoul, H., Motahhir, S., Ait abdelmoula, I., Aniba, G.: Optimized topology for a photovoltaic array using switches control. *Energy Conversion and Management* **291** (September 2023) 117315
5. Sreekantha Reddy, S., Yammani, C.: Parameter extraction of single-diode photovoltaic module using experimental current–voltage data. *International Journal of Circuit Theory and Applications* **50**(2) (2022) 753–771 .eprint: <https://onlinelibrary.wiley.com/doi/pdf/10.1002/cta.3133>.
6. Sharma, A., Sharma, A., Averbukh, M., Jatly, V., Rajput, S., Azzopardi, B., Lim, W.H.: Performance investigation of state-of-the-art metaheuristic techniques for parameter extraction of solar cells/module. *Scientific Reports* **13**(1) (July 2023) 11134 Publisher: Nature Publishing Group.
7. Ridha, H.M.: Parameters extraction of single and double diodes photovoltaic models using Marine Predators Algorithm and Lambert W function. *Solar Energy* **209** (October 2020) 674–693
8. Batzelis, E.: Non-Iterative Methods for the Extraction of the Single-Diode Model Parameters of Photovoltaic Modules: A Review and Comparative Assessment. *Energies* **12**(3) (January 2019) 358 Number: 3 Publisher: Multidisciplinary Digital Publishing Institute.
9. Dali, A., Bouharchouche, A., Diaf, S.: Parameter identification of photovoltaic cell/module using genetic algorithm (GA) and particle swarm optimization (PSO). In: 2015 3rd International Conference on Control, Engineering & Information Technology (CEIT). (May 2015) 1–6
10. Liang, J., Ge, S., Qu, B., Yu, K., Liu, F., Yang, H., Wei, P., Li, Z.: Classified perturbation mutation based particle swarm optimization algorithm for parameters extraction of photovoltaic models. *Energy Conversion and Management* **203** (January 2020) 112138

11. Li, S., Gong, W., Yan, X., Hu, C., Bai, D., Wang, L.: Parameter estimation of photovoltaic models with memetic adaptive differential evolution. *Solar Energy* **190** (September 2019) 465–474
12. Ishaque, K., Salam, Z.: An improved modeling method to determine the model parameters of photovoltaic (PV) modules using differential evolution (DE). *Solar Energy* **85**(9) (September 2011) 2349–2359
13. Oufettoul, H., Motahhir, S., Abdelmoula, I., Aniba, G., Issa, W., Mahir, O.: Optimum MPPT Technique for Reconfiguring the Photovoltaic Array Under Partial Shading Failure. (August 2023) Pages: 338.
14. Yaqoob, S.J., Motahhir, S., Agyekum, E.B.: A new model for a photovoltaic panel using Proteus software tool under arbitrary environmental conditions. *Journal of Cleaner Production* **333** (January 2022) 130074
15. Premkumar, M., Subramaniam, U., Babu, T.S., Elavarasan, R.M., Mihet-Popa, L.: Evaluation of Mathematical Model to Characterize the Performance of Conventional and Hybrid PV Array Topologies under Static and Dynamic Shading Patterns. *Energies* **13**(12) (January 2020) 3216 Number: 12 Publisher: Multidisciplinary Digital Publishing Institute.
16. Mirjalili, S., Mirjalili, S.M., Lewis, A.: Grey Wolf Optimizer. *Advances in Engineering Software* **69** (March 2014) 46–61